- Supplemental data -

Dissecting the molecular effects of cigarette smoke on proteasome function

SUPPLEMENTAL METHODS

SDS-polyacrylamide gel electrophoresis: SDS-PAGE gels were prepared using 10 % or 12 % acrylamide. Silver stains of isolated 26S fractions were performed with a Pierce® Silver Stain kit (Thermo Scientific). Coomassie staining of isolated 20S proteasomes was performed using InstantBlue staining solution (Expedeon).

Proteasome activity assays: Luminogenic substrates used for determination of CT-L, T-L, and C-L activities of purified 26S complexes and cell extracts were Succinyl-leucine-leucine-valine-tyrosine-aminoluciferin (Suc-LLVY-aminoluciferin), Z-leucine-arginine-arginine-aminoluciferin (Z-LRR-aminoluciferin), and Z-norleucine-proline-norleucine-aspartate-aminoluciferin (Z-nLPnLD-aminoluciferin), respectively (Proteasome-Glo™ Assay System, Promega). Assays were performed in white flat bottom 96-well plates (BD Falcon) and according to the manufacturer's instructions. Luminescence was measured in a Tristar LB 941 plate reader (Berthold Technologies). Blank luminescence values were subtracted from each well.

Isolation of 26S proteasome complexes:
His_{10}-UIM (S5a) expression and purification: E. *coli* strain Rosetta2 (DE3) was transformed with the pET-26b(+)/S5a (196-306) construct and cultured at 20 °C in two 2-L flasks, containing 500 mL of ZYM 5052 auto-induction medium [1], 30 μg/mL of kanamycin, and 33 μg/mL of chloramphenicol. Cells were harvested by centrifugation after reaching saturation, resuspended in 30 mL of lysis buffer (20 mM sodium phosphate, 300 mM NaCl, 20 mM imidazole, 10 mM $MgSO_4$, 10 μg/mL DNase I, 1 mM AEBSF.HCl, pH 7.5), and lysed by sonication. Lysates were centrifuged (40,000 x *g*) and filtered (0.2 μm). The supernatant was applied to a 5-mL HiTrap Chelating HP column (GE Healthcare), previously equilibrated in buffer A (20 mM sodium phosphate, 300 mM NaCl, 20 mM imidazole, pH 7.5) using an Äkta Purifier (GE Healthcare). The column was washed with buffer A, and buffer A containing 50 mM of imidazole until a stable baseline was reached (monitored at 280 nm). Bound proteins were eluted with buffer B (20 mM sodium phosphate, 300 mM NaCl, 300 mM imidazole, pH 7.5) and fractions containing protein were pooled and concentrated to less than 5 mL. This was subsequently applied to size exclusion chromatography, using a HiLoad 16/600 Superdex 200 column (GE Healthcare), equilibrated in buffer C (20 mM sodium phosphate, 300 mM NaCl, pH 7.5). Fractions containing S5a were collected, diluted with buffer C to approximately 10 mg/mL, flash frozen in liquid nitrogen in 250 μL aliquots and stored at -80 °C.
GST-UBL expression and purification: Expression and purification of glutathione-transferase-tagged ubiquitin-like domain (GST-UBL) were performed as described [2]. *E. coli* strain BL21 AI was transformed with the DEST15-UBL-HHR23B construct and cultured at 37 °C in four 2-L flasks containing 500 mL of LB medium and 100 μg/mL of ampicillin. Protein expression was induced by the addition of 0.1 % of L-arabinose, when cultures reached an optical density at

600 nm of 0.6. Cultures were further incubated for 3 h at 37 °C. Cells were harvested by centrifugation, re-suspended in 50 mL lysis buffer (PBS, 10 mM $MgCl_2$, 10 µg/mL DNase I, 2 mM ATP, 1 mM DTT), and lysed by sonication. Lysates were centrifuged (40,000 x *g*) and filtered (0.2 µm). The supernatant was applied to a 5-mL GSTrap column (GE Healthcare), equilibrated with PBS using an Äkta Purifier (GE Healthcare). The column was washed with PBS and bound proteins were eluted with the elution buffer (100 mM Tris, 100 mM NaCl, 20 mM reduced glutathione, 1 mM DTT, pH 8.0). Fractions containing protein were pooled and dialyzed overnight at 4 °C against 1 L storage buffer (25 mM HEPES, 5 mM $MgCl_2$, 1 mM DTT, 10 % (v/v) glycerol, pH 7.2). The protein was diluted with storage buffer to approx. 10 mg/mL, flash frozen in liquid nitrogen in 250-µL aliquots and stored at -80 °C.

26S proteasome complexes were isolated from A549 cells and from mouse lung homogenates as described [2]. For each purification from A549, 5×10^6 cells were seeded in five 15 cm dishes. When reaching 80 % confluency, cells were trypsinized, washed twice with PBS, and harvested by centrifugation. Cell pellets were resuspended in lysis buffer (20 mM HEPES pH 7.2, 0.32 M Sucrose, 5 mM $MgCl_2$, 0.2 % NP-40, 0.05 % NaN_3, 2 mM ATP, and cOmplete™ protease inhibitor cocktail from Roche), and homogenized using the Micro-Dismembrator (Sartorius Stedim Biotech).

Mouse lungs were homogenized (Micro-Dismembrator) in 500 µL of distilled water containing protease inhibitor cocktail (cOmplete™, Roche) and lysed under hypo-osmotic lysis conditions by five cycles of repeated freezing (liquid nitrogen) and thawing (water bath, 37 °C). After removal of debris by centrifugation (14,000 × *g*, 4 °C), supernatants were used for determination of protein concentrations (Pierce BCA kit, Thermo Scientific), proteasome activity, and isolation of 26S complexes.

Cell and lung homogenates were incubated with Glutathione-Sepharose™ 4B (GE Healthcare, 250 µL/mg GST-UBL) and either with GST-UBL (0.2 mg/mL lysate) for 26S isolation or GST alone (Thermo Scientific, 0.2 mg/mL lysate) for pull-down controls for 2 h at 4 °C. After being washed extensively (3 x 25 mL of purification buffer), the GSH Sepharose resin was gently agitated twice in 1 bed volume of 2 mg/mL His_{10}-UIM (S5a) for 15 min. Eluted fractions were pooled and incubated for 20 min with pre-equilibrated Ni-NTA (Thermo Scientific, 100 µL/mg His_{10}-UIM) to remove excess of His_{10}-UIM. Final eluted fractions, containing purified 26S complexes, were collected by spinning samples through a 0.22-µm filter (Millipore), supplemented with 35 % glycerol and stored at -20 °C. Protein concentration of isolated 26S complexes was determined with a Bio-Rad Protein Assay (Bio-Rad).

Label-free LC-MS/MS analysis of isolated 26S proteasome complexes: Prior to MS analyses, isolated 26S samples and pull-down controls were precipitated by four volumes of chilled acetone. The mixture was vortexed and incubated overnight at -20 °C. The next day, the mixture was vortexed and centrifuged (15,000 x *g*, 20 min). Supernatant was discarded and pellet was air-dried at RT.

Precipitated proteins were resuspended in 20 µL of 50 mM ammonium bicarbonate and cysteine residues were reduced using 1 µL of 100 mM DTT at 60 °C for 10 min. After acetylation, using 1 µL of 300 mM iodacetamide for 30 min at RT in the dark, samples were digested in-solution with 2 µg of trypsin (Sigma) overnight at 37 °C. Samples were acidified with 0.5 % trifluoroacetic acid (TFA) and stored at -20 °C.

Before loading, samples were centrifuged for 5 min at 4 °C. LC-MS/MS analysis was performed as described previously [3] on a LTQ-OrbitrapXL (Thermo Fisher Scientific Inc.) online coupled to an Ultimate 3000 nano-HPLC (Dionex). Samples were injected and loaded onto the trap column (300 µm inner diameter × 5 mm, packed with Acclaim PepMap100 C18, 5 µm, 100 Å; LC Packings, Sunnyvale, CA) at a flow rate of 30 µL/min in 0.1 % TFA. After 5 min, peptides were eluted from the trap column and separated on a C18 analytical column (PepMap, 25 cm, 75µm ID, 2 µm/100 Å pore size, LC Packings) by a 135 min gradient from 5 % to 50 % of buffer B (75 % acetonitrile (ACN)/ 0.1 % formic acid (FA) in HPLC-grade water) in buffer A (2 % ACN / 0.1 % FA in HPLC-grade water) at 300 nL/min flow rate, followed by a short gradient from 50 % to 95 % buffer B in 5 min. Between each sample, the gradient was set back to 5 % buffer B and left to equilibrate for 20 min. From the MS prescan, the 10 most abundant peptide ions were selected for fragmentation in the linear ion trap if they exceeded an intensity of at least 200 counts and if they were at least doubly charged. During fragment analysis, a high-resolution (60,000 full-width half maximum) MS spectrum was acquired in the Orbitrap with a mass range from 300 Da to 1,500 Da.

The mass spectrometry data of the proteasome pull-downs have been deposited to the ProteomeXchange Consortium via the PRIDE partner repository [4] with the dataset identifier PXD007148. The proteome data published in Mossina *et al.* [5] can be found with the dataset identifier PXD007180.

The acquired spectra were loaded to the Progenesis QI software (version 3.0, Nonlinear Dynamics, Waters, Newcastle upon Tyne, U.K.) for label-free quantification and analyzed as described previously [3,6]. Briefly, profile data of the MS scans were transformed to peak lists with respective peak *m/z* values, intensities, abundances (areas under the peaks) and *m/z* width. MS/MS spectra were treated similarly. After reference selection, the retention times of the other samples were aligned by manual and automatic alignment to a maximal overlay of all features. Features with one charge or more than seven charges were excluded from further analyses. No minimal thresholds were set neither for the method of peak picking nor selection of data to use for quantification. All MS/MS spectra were exported as Mascot generic file and used for peptide identification with Mascot (version 2.6.0., MatrixScience, London, UK) in the Swissprot human (Release 2017_02, 20194 sequences. 11329970 residues) or Swissprot mouse protein database (Release 2017_02, 16868 sequences. 9511662 residues). Search parameters were as follows: mass tolerance was 10 ppm peptide and 0.6 Da fragment; one missed cleavage was allowed, carbamidomethylation was set as fixed modification; methionine oxidation and asparagine or glutamine deamidation were allowed as variable modifications. A Mascot-integrated decoy database search calculated an average false discovery of < 1 % when searches were performed

with the Mascot percolator score setting and a significance threshold $p < 0.05$. Peptide assignments were re-imported into the Progenesis QI software and the abundances of all peptides allocated to each protein were summed up. Raw abundances were used for calculation of enrichment factors of proteins comparing the three GST controls with the 26S proteasome pull-downs. Even though not all peptides were detected in the GST controls, numeric abundance values were assigned to allow for quantification. Normalized abundances were used for calculation of fold changes of proteins comparing the 26S proteasome pull-downs between cigarette smoke treated and untreated samples. An enrichment ratio cut-off of 3 and a significance threshold $p < 0.05$ (Student's *t*-test) was used for the selection of specific proteins.

Stoichiometry calculations and plot generation: For calculation of protein stoichiometries, the abundances of the three most abundant peptides per protein were summed up and referenced to the bait protein PSMD4 (TOP3 method [7]). The three most abundant peptides for PSMD4 itself were selected manually, rejecting peptides from overlapping regions with His_{10}-UIM, which was artificially introduced during the purification procedure. Stoichiometry plots were generated comparing the stoichiometries in the 26S pull-down samples (interaction stoichiometry) with stoichiometries in cell extracts (abundance stoichiometry) [5,8].

Isolation of the 20S proteasome complexes:
Twenty 15 cm dishes (80-90 % confluent) of control or CSE-treated HEK293 cells stably expressing a FLAG-tagged β4 subunit were collected, snap-frozen and stored at -80 °C. Cell pellets were resuspended in 8 mL of lysis buffer (50 mM Tris pH 7.5, 150 mM NaCl, 0.5 % NP-40, 5 mM $MgCl_2$, supplemented for the lysis step with protease and phosphatase inhibitors (5 mM Na-o-vanadate, 4 mM Na-pyrophosphate, 4 mM β-glycerophosphate, 1 mM PMSF, 1 mM benzamidine, 1.4 µg/ml pepstatin A) and incubated for 10 min at 4 °C rotating. Lysates were carefully homogenized using a glass homogenizer with 40 strokes and cleared by centrifugation with 14,000 x *g* for 10 min at 4 °C. Meanwhile, columns (Poly-Prep Chromatography Columns, Bio-Rad) were prepared and loaded with 1 mL anti-FLAG M2 affinity gel (Sigma-Aldrich), the liquid was allowed to drain by gravity flow. The beads were washed with 5 mL lysis buffer (without protease and phosphatase inhibitors), 5 mL 100 mM glycine (pH 3.5), and again 10 mL lysis buffer. Afterwards, the column drain was closed, the beads were resuspended in 1 mL lysis buffer and the cleared lysate was applied to the column. The column was incubated for 90 min at 4 °C while rotating. After incubation, the liquid in the column was allowed to drain and the beads were washed with 50 mL lysis buffer. The column was closed again and beads were incubated in 5 mL lysis buffer supplemented with 500 mM NaCl for 1 h at 4 °C while rotating. Afterwards, the liquid was allowed to drain and the beads were washed with 4 mL lysis buffer, then washed with 40 mL of 500 mM ammonium acetate. For elution, 1 mL elution buffer (500 mM ammonium acetate, 0.5 mg/mL FLAG peptide) was added to the beads and reapplied for a second elution. This was repeated for four times in total to collect 4 mL eluate. The eluate was

concentrated with an Amicon Ultra centrifugal filter with a cutoff of 30 kDa to approx. 150 µl final volume. Isolated 20S proteasomes were aliquoted to 5 µL, snap-frozen and stored at -80 °C.

Native MS analysis of 20S proteasome complexes:
Native MS experiments were performed using a Q Exactive™ Plus mass spectrometer (Thermo Fisher Scientific) modified for the transmission, detection, and fragmentation of high *m/z* ions [9]. All spectra were calibrated externally, using cesium iodide and data is presented without smoothing. Data analysis was performed using Thermo Xcalibur 3.0.63, 2013. Typically, 2-3 µL of protein solution was loaded into a gold-coated nano-ESI capillary prepared in-house, as previously described [10], and sprayed into the instrument. Conditions within the mass spectrometer were adjusted to preserve non-covalent interactions, with the source operating in positive mode. Experimental parameters used were as follows: capillary voltage 1.7 kV, inlet capillary temperature 180 °C, bent flatapole DC 2.2 V, axial gradient 37.2 V and argon was used as the collision gas in the HCD cell. For the measurement of the intact 20S proteasome, spectra were recorded at a resolving power of 10,000. To facilitate dissociation of the 20S into composing subunits, the HCD cell bias was set between 0 to -200 V. Trapping gas pressure was set to 3.9, corresponding to pressures of 1.23×10^{-4} and 5.27×10^{-10} mbar, in the HV and UHV regions, respectively. To measure the masses of the dissociated subunits, spectra were recorded at a resolving power of 20,000. Bent flatapole DC bias was 1.8 V, axial gradient 16.8 V and HCD cell bias 200 V. Trapping gas pressure was set to 1.5, corresponding to pressures of 4.75×10^{-5} and 3.37×10^{-10} mbar, in the HV and UHV regions, respectively.

LC/MS analysis of 20S proteasome complexes: LC/MS analysis of purified 20S proteasomes was performed as described in [11]. In brief, reverse phase liquid chromatography was performed with a nUPLC system, using a monolithic column prepared in-house. About 3 µg of protein were loaded onto the column and eluted using a linear gradient of 20 % to 60 % ACN, complemented with 0.05 % FA and 0.035 % TFA, over 30 min, at a flow rate of 15 µL/min, at 60 °C. Eluted proteins were analyzed on-line by a QStar XL mass spectrometer, using the following experimental parameters: capillary 5.8 kV, declustering potential of 40 V, focusing potential of 200 V, and second declustering potential of 20 V. The mass range was defined as 500–5000 *m/z*. Spectra were calibrated using a solution of Reserpine. No smoothing was applied to the spectra. Data was analyzed using Analyst QS 2.0 2005.

SUPPLEMENTAL FIGURES

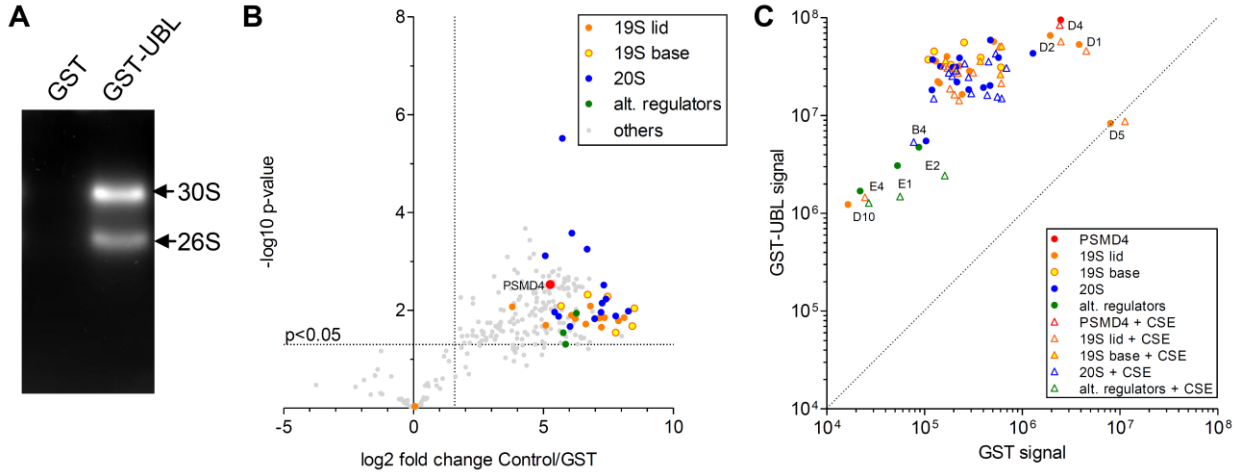

Figure S1: Quality control of PSMD4 pull-down. (A) Equal protein amounts (10 µg) were loaded onto native gels from pull-down samples obtained with GST or GST-UBL (ubiquitin-like domain derived from hHR23B). Gels were incubated with Suc-LLVY-AMC, a fluorogenic substrate of the chymotrypsin-like activity, and imaged under UV-light. **(B)** Enrichment analysis of detected GST-UBL pull-down proteins by mass spectrometry of samples from control A549 cells over GST pull-down in three individual samples. All 20S and 19S proteasome subunits were significantly enriched, as well as regulators PA28α, PA28β, and PA28γ (PSME1-PSME3). PSMD5, an assembly chaperone of 19S, was not enriched over GST control. Further analysis was performed on those proteins that were significantly enriched at least threefold over GST in control or CSE-treated cells (Student's *t*-test, *p*-values < 0.05 were considered statistically significant). **(C)** Proteasome subunits' pull-down enrichment signal (GST-UBL, y-axis) over background GST signal (x-axis).

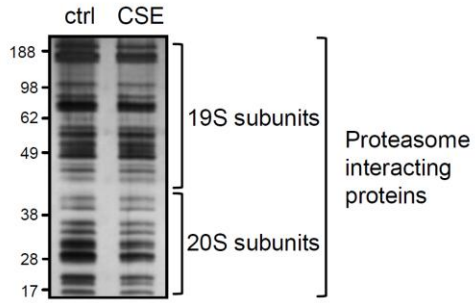

Figure S2: Protein pattern of pull-down samples. Equal protein amounts of pull-down samples derived from control A549 cells or cells exposed to 25 % CSE for 24 h were separated on SDS-gels and silver-stained. The typical pattern of 20S, 19S proteins and proteasome interacting proteins (PIPs) was observed as previously described [2].

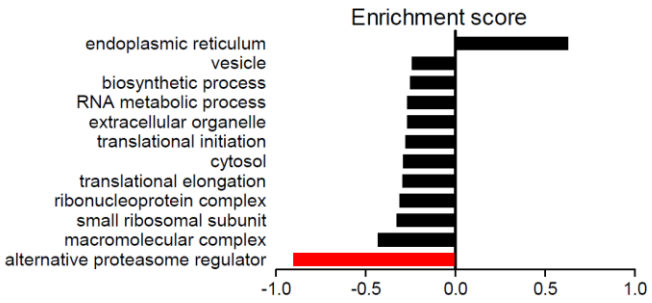

Figure S3: Gene ontology analysis of isolated 26S proteasome complexes. 26S proteasome complexes were isolated from A549 cells treated with 25 % cigarette smoke extract (CSE) for 24 h normalized to control (ctrl). GO analysis was performed on all identified proteins, only annotations with significant regulation are shown. Self-defined annotation "alternative proteasome regulator" indicated in red comprises PSME1, PSME2 and PSME4.

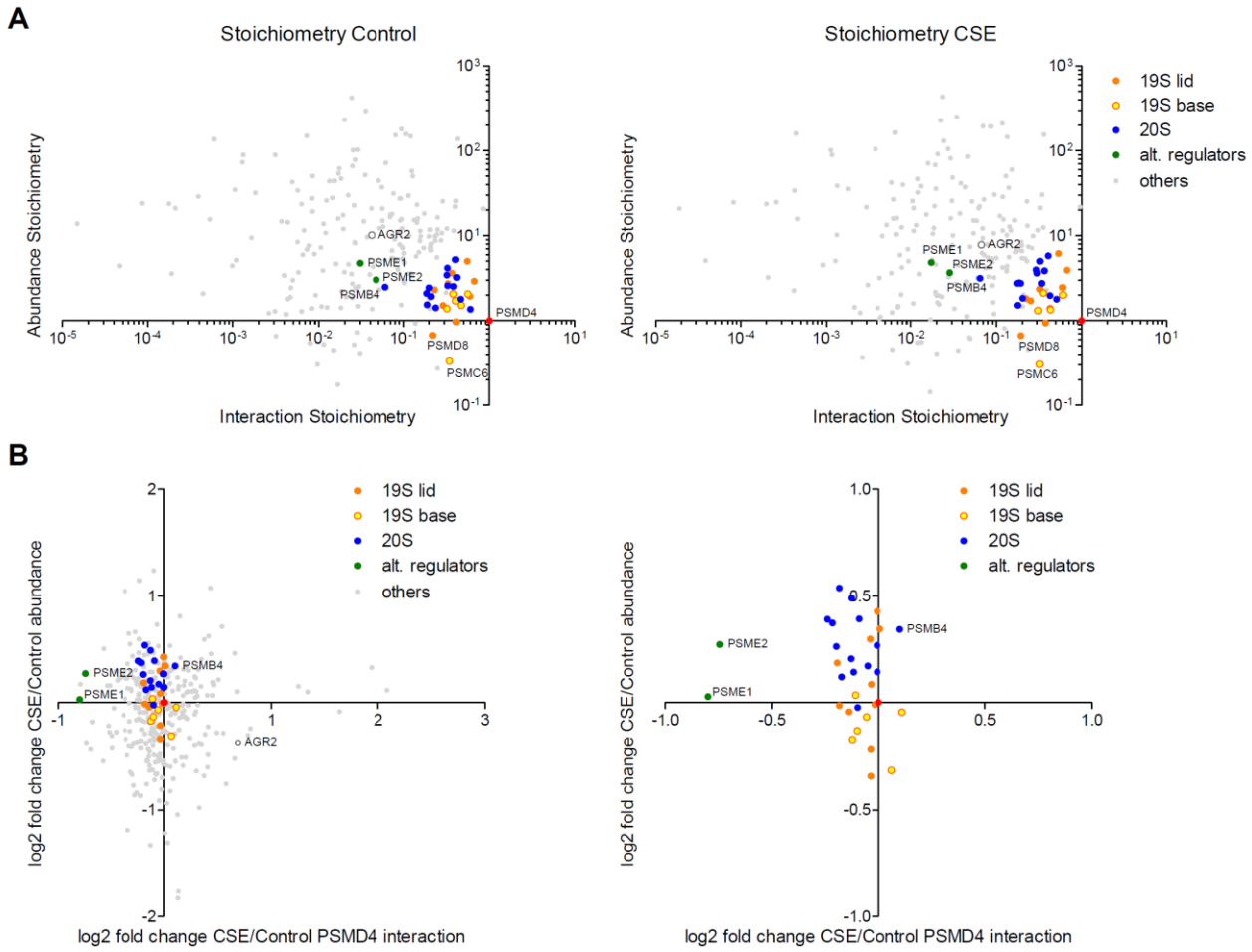

Figure S4: Stoichiometry analysis of pull-down proteins. (A) Abundance of proteins in whole proteome analysis (see Figure 1) or in PSMD4 pull-down of control A549 cells and CSE-treated cells (see Figure 2C) are displayed relative to PSMD4. Only the proteins detected in both datasets were examined. Note that regulators PSME1 and PSME2 (associated with 20S immunoproteasomes, green) are comparable in abundance to PSMD4, but interact much less than other 20S or 19S subunits. AGR2, the only protein significantly enriched in the pull-down, is highlighted. (B) Combined plot of fold change for all identified proteins (left) and zoom-in on proteasome subunits (right) in response to cigarette smoke and relative to PSMD4.

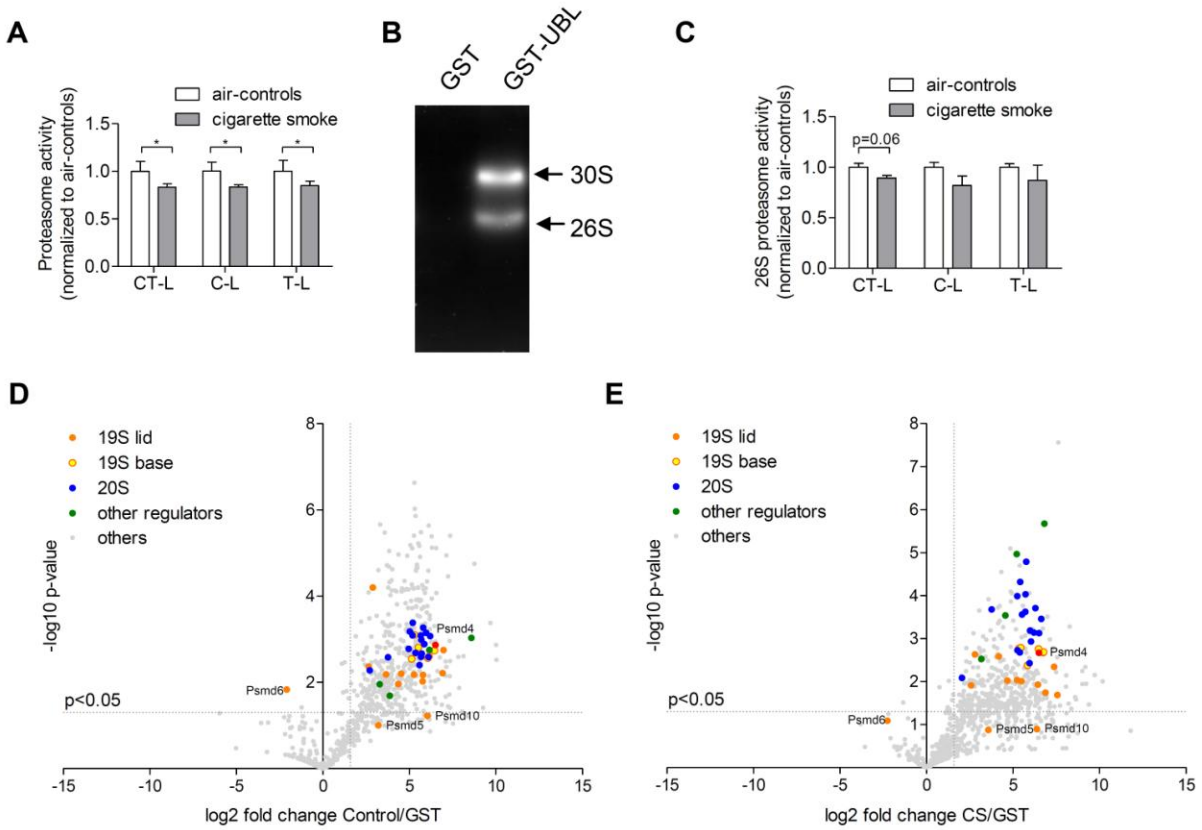

Figure S5: Proteasome activity and pull-down quality control in lungs of cigarette smoke-exposed mice. Mice were exposed to cigarette smoke for three days with two exposure cycles of 50 min/day. On the fourth day, lungs were perfused with PBS, harvested and snap-frozen. **(A)** The three different proteasome activities of native lung lysates from air-controls or cigarette smoke (CS)-exposed mice (15 individual mice per group) were measured with luminogenic substrates. Displayed are mean + SEM values normalized to air-controls (Student's *t*-test, * = $p < 0.05$). **(B)** Pull-down of proteasome complexes from murine lungs with GST alone or with GST-UBL (ubiquitin-like domain derived from hHR23B): Equal protein amounts (10 µg) were loaded onto native gels from pull-down samples and proteasome activity was assessed: The gel was incubated with Suc-LLVY-AMC, a fluorogenic substrate of the chymotrypsin-like activity, and imaged under UV-light. The upper band corresponds to 20S with 19S regulators attached to one or to both sides, respectively. The lower bands depict 20S proteasomes with attached 11S regulators or PA200. **(C)** Activities of PSMD4 pull-down proteasome complexes from lungs exposed to cigarette smoke or controls were measured with luminogenic substrates. Displayed are mean + SEM values normalized to air-controls (n = 3 pools of 4 individual mice each per group, Student's *t*-test, *p*-values < 0.05 were considered statistically significant). **(D and E)** Enrichment analysis of detected GST-UBL pull-down proteins by MS over GST pull-down in three individual samples from smoke-exposed mouse lungs or controls (n = 3, four lungs pooled per sample, same samples as in (C)). All 20S and most 19S proteasome subunits were significantly enriched as well as regulators PA28α, PA28β, and PA28γ (Psme1-Psme3). Psmd5,

Psmd6, and Psmd10 were not significantly enriched and therefore not considered in further analysis. Only those proteins that were significantly enriched at least threefold over GST in control or CSE-treated cells were considered. (Student's *t*-test, *p*-values < 0.05 were considered statistically significant).

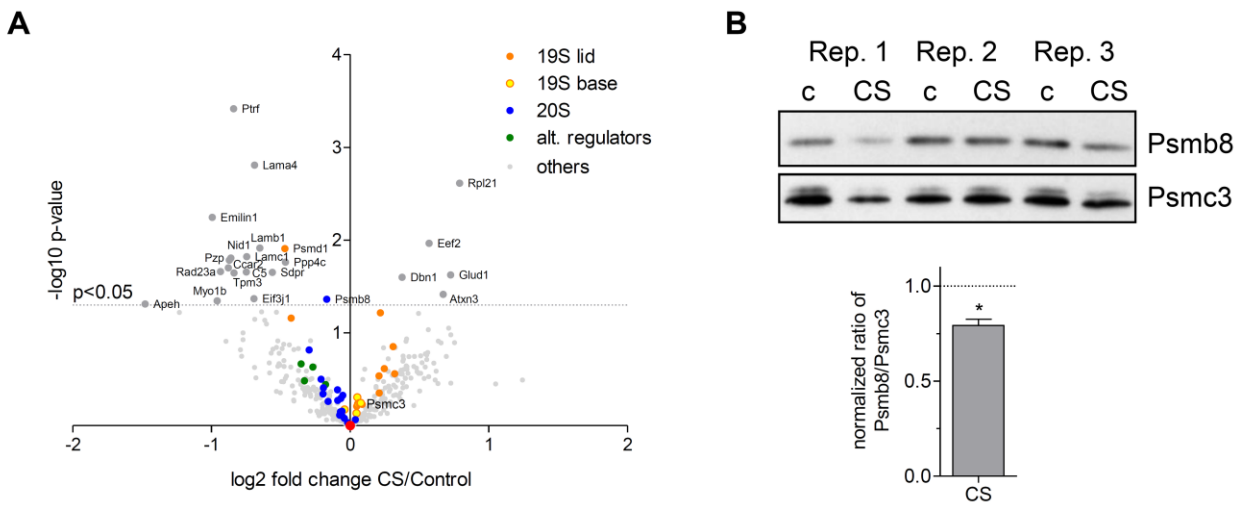

Figure S6: Interactome analysis of isolated 26S proteasomes from mouse lungs. (A) Differential interactome of proteasome complexes from lungs exposed to cigarette smoke compared to controls. Association of five proteins was significantly enhanced in response to cigarette smoke, 18 were associated less (Student's *t*-test, *p*-values < 0.05 were considered statistically significant, see also Supplemental Table S2). **(B)** Verification of reduced Psmb8 in CS-treated samples compared to Psmc3. WB analysis of the three replicates, data from densitometric analysis were normalized to their controls (One sample *t*-test, *p*-values < 0.05 were considered statistically significant).

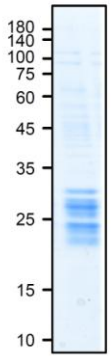

Figure S7: 20S pull-down in HEK293 cells expressing FLAG-tagged β4 subunit. Eluted 20S proteasome was subjected to SDS-gel analysis with Coomassie staining. The typical pattern of 20S protein bands between 20 and 35 kDa can be observed.

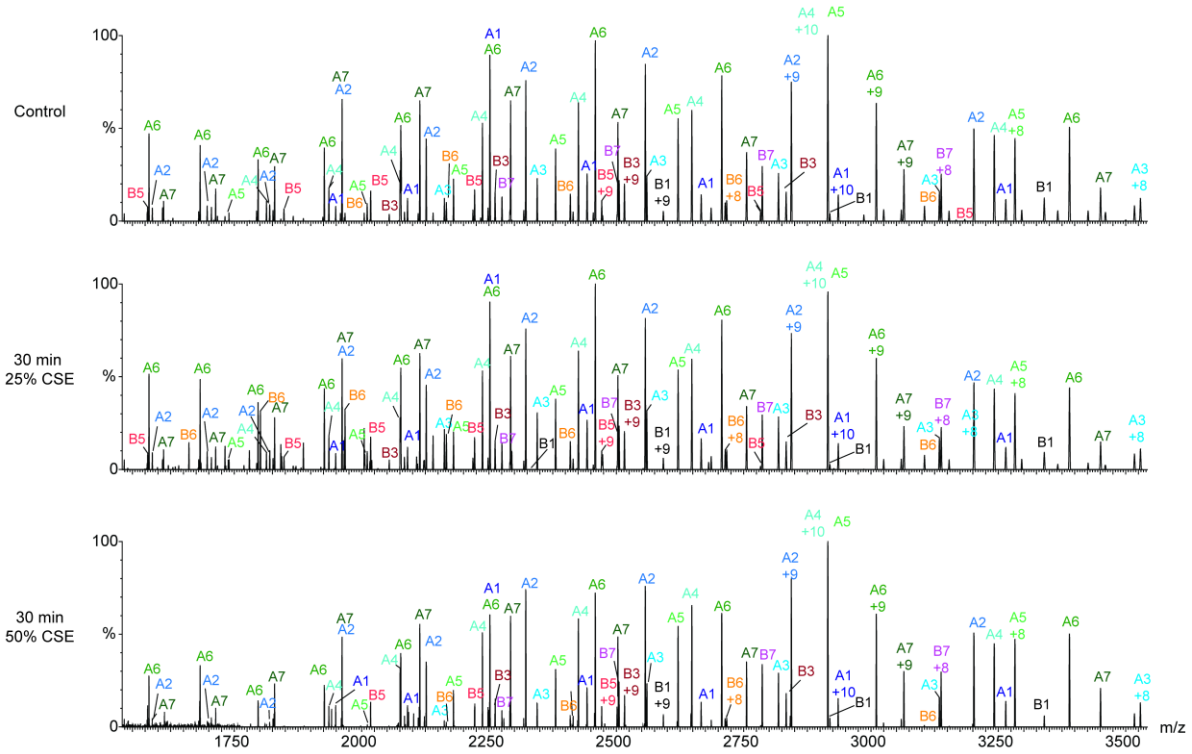

Figure S8: Analysis of 20S proteasome subunits purified from cells exposed to different CSE treatments did not reveal novel PTMs. Isolated 20S proteasomes were measured at conditions optimized for full dissociation of the complexes into their composing subunits. Measured masses and their corresponding proteoforms are shown in Table 1.

SUPPLEMENTAL TABLE

Table S1: GO enrichment analysis from proteomic data of A549 cells treated with cigarette smoke ranked by enrichment score.

Type	Name	Size	Score	P value	Benj. Hoch. FDR	Mean	Median
Annotation_sub	**20S proteasome**	14	0.65690	2.23E-05	8.94E-05	0.33718	0.32917
GOMF name	threonine-type endopeptidase activity	14	0.65690	2.23E-05	0.00394	0.33718	0.32917
GOMF name	threonine-type peptidase activity	14	0.65690	2.23E-05	0.00359	0.33718	0.32917
GOCC slim name	microvillus	11	0.45210	9.63E-03	0.05973	0.26077	0.32187
Annotation_Proteasome	**Proteasome subunits**	34	0.40281	5.58E-05	5.58E-05	0.20891	0.23059
GOMF name	protein transporter activity	22	0.39632	1.38E-03	0.09334	0.22092	0.21366
GOCC slim name	**proteasome complex**	42	0.39215	1.36E-05	0.00028	0.20054	0.21545
GOBP slim name	xenobiotic metabolic process	21	0.35362	5.27E-03	0.05560	0.17074	0.18938
GOCC slim name	nuclear pore	15	0.34911	1.97E-02	0.09776	0.17920	0.21250
GOCC slim name	small nuclear ribonucleoprotein complex	25	0.34814	2.75E-03	0.02440	0.28392	0.30413
GOCC slim name	microbody	22	0.30951	1.25E-02	0.06717	0.15670	0.16424
GOBP slim name	protein folding	85	0.26393	3.85E-05	0.00091	0.12328	0.17366
GOBP slim name	mitochondrion organization	54	0.25738	1.25E-03	0.01781	0.12375	0.17401
GOCC slim name	intracellular	34	0.25260	1.15E-02	0.06482	0.12442	0.12713
GOCC slim name	cell part	1778	0.22607	3.38E-04	0.00465	-0.01463	0.02544
GOBP slim name	**proteolysis involved in cellular protein catabolic process**	85	0.21834	6.61E-04	0.01046	0.10260	0.14525
GOMF name	oxidoreductase activity	138	0.16817	9.95E-04	0.07026	0.07976	0.10804
GOBP slim name	protein modification by small protein conjugation or removal	90	0.16692	7.47E-03	0.07343	0.07363	0.12169
GOBP slim name	nucleobase-containing small molecule metabolic process	89	0.16051	1.05E-02	0.08806	0.07478	0.09464
GOBP slim name	heterocycle metabolic process	106	0.15443	7.50E-03	0.07126	0.07623	0.09382
GOCC slim name	cytosol	665	0.15340	3.90E-08	1.61E-06	0.05055	0.07438
GOBP slim name	mitotic cell cycle	95	0.15285	1.20E-02	0.09214	0.07635	0.07955
GOCC slim name	endoplasmic reticulum	137	0.13503	8.43E-03	0.05501	0.06000	0.08404
GOBP slim name	**proteolysis**	123	0.13410	1.28E-02	0.09364	0.04607	0.10914
GOCC slim name	mitochondrion	262	0.13254	5.73E-04	0.00646	0.05620	0.06879
GOBP slim name	small molecule metabolic process	439	0.12192	1.10E-04	0.00240	0.04048	0.06684
GOCC slim name	cytoplasm	814	0.11287	2.83E-05	0.00050	0.02339	0.05273

Type	Name	Size	Score	P value	Benj. Hoch. FDR	Mean	Median
GOCC slim name	extracellular organelle	896	0.09366	4.65E-04	0.00577	0.00211	0.06588
GOBP slim name	catabolic process	341	0.09242	7.55E-03	0.06943	0.03325	0.07185
GOCC slim name	intracellular organelle	1270	0.08378	3.48E-03	0.02875	-0.00128	0.02997
GOCC slim name	intracellular membrane-bounded organelle	1106	0.08203	2.57E-03	0.02455	0.00101	0.03348
GOCC slim name	vesicle	940	0.07530	4.86E-03	0.03768	-0.00598	0.05824
GOBP slim name	macromolecule metabolic process	961	-0.07865	3.28E-03	0.03596	-0.04595	-0.01415
GOCC slim name	plasma membrane	364	-0.08659	1.03E-02	0.06067	-0.07278	-0.03242
GOBP slim name	RNA metabolic process	456	-0.09354	2.64E-03	0.03138	-0.04996	-0.08561
GOBP slim name	cellular process	1629	-0.10211	1.10E-02	0.08944	-0.03062	0.01027
GOMF name	binding	1345	-0.10651	3.51E-04	0.03446	-0.04313	-0.00488
GOBP slim name	multicellular organismal process	320	-0.12310	5.19E-04	0.00924	-0.11249	-0.02622
GOBP slim name	cellular component disassembly	165	-0.14698	1.80E-03	0.02444	-0.10640	-0.11101
GOBP slim name	regulation of body fluid levels	108	-0.15113	8.30E-03	0.07390	-0.14088	-0.07772
GOBP slim name	chromosome organization	103	-0.15883	6.67E-03	0.06786	-0.10764	-0.08651
GOBP slim name	multi-organism process	87	-0.15987	1.17E-02	0.09261	-0.12126	-0.07000
GOCC slim name	extracellular space	210	-0.16903	6.45E-05	0.00100	-0.15677	-0.07826
GOBP slim name	anatomical structure morphogenesis	161	-0.17255	2.90E-04	0.00591	-0.13892	-0.06770
GOBP slim name	chromatin organization	77	-0.17384	9.70E-03	0.08377	-0.10646	-0.10981
GOBP slim name	response to external stimulus	185	-0.20563	4.29E-06	0.00015	-0.16067	-0.09316
GOBP slim name	cellular component movement	160	-0.20975	1.12E-05	0.00035	-0.16014	-0.08280
GOMF name	transferase activity, transferring phosphorus-containing groups	65	-0.23027	1.59E-03	0.09660	-0.17159	-0.13851
GOMF name	molecular transducer activity	65	-0.24802	6.70E-04	0.05139	-0.18511	-0.19144
GOMF name	signal transducer activity	65	-0.24802	6.70E-04	0.04925	-0.18511	-0.19144
GOBP slim name	polysaccharide metabolic process	34	-0.24997	1.24E-02	0.09294	-0.20070	-0.14525
GOMF name	kinase activity	52	-0.25672	1.57E-03	0.09924	-0.19089	-0.15448
GOCC slim name	chromosome	30	-0.26220	1.36E-02	0.07045	-0.18452	-0.14735
GOBP slim name	protein phosphorylation	55	-0.27152	5.92E-04	0.00993	-0.20657	-0.19144
GOBP slim name	locomotion	171	-0.27685	2.30E-09	1.31E-07	-0.20831	-0.14358
GOCC slim name	synapse	31	-0.28477	6.48E-03	0.04462	-0.23511	-0.23577
GOBP slim name	anatomical structure formation involved in morphogenesis	88	-0.29049	4.10E-06	0.00017	-0.21748	-0.19705
GOBP slim name	regulation of mitotic cell cycle	41	-0.29711	1.12E-03	0.01684	-0.21959	-0.20770

Type	Name	Size	Score	P value	Benj. Hoch. FDR	Mean	Median
GOBP slim name	cell motility	108	-0.29899	1.77E-07	8.39E-06	-0.23070	-0.17075
GOBP slim name	cell junction organization	47	-0.30446	3.59E-04	0.00682	-0.24942	-0.16977
GOBP slim name	growth	34	-0.30863	2.02E-03	0.02613	-0.25079	-0.35824
GOBP slim name	embryo development	31	-0.31933	2.27E-03	0.02808	-0.24023	-0.18102
GOCC slim name	cell surface	88	-0.33205	1.40E-07	4.35E-06	-0.23975	-0.32347
GOMF name	glycosaminoglycan binding	31	-0.33283	1.46E-03	0.09559	-0.31670	-0.40248
GOCC slim name	receptor complex	22	-0.34308	5.61E-03	0.04089	-0.27754	-0.50129
GOCC slim name	extracellular region	146	-0.35072	1.85E-12	2.30E-10	-0.29832	-0.32109
GOMF name	pattern binding	33	-0.36107	3.71E-04	0.03276	-0.33034	-0.41735
GOMF name	polysaccharide binding	33	-0.36107	3.71E-04	0.03120	-0.33034	-0.41735
GOMF name	peptidase regulator activity	47	-0.36231	2.17E-05	0.00426	-0.27817	-0.24999
GOMF name	endopeptidase regulator activity	38	-0.38308	5.18E-05	0.00704	-0.30028	-0.36147
GOMF name	growth factor binding	25	-0.42405	2.66E-04	0.02930	-0.36234	-0.42201
GOBP slim name	cell morphogenesis	33	-0.43269	1.99E-05	0.00052	-0.32963	-0.37587
GOMF name	endopeptidase inhibitor activity	35	-0.43537	9.96E-06	0.00293	-0.33605	-0.40248
GOMF name	peptidase inhibitor activity	35	-0.43537	9.96E-06	0.00251	-0.33605	-0.40248
GOMF name	receptor activity	65	-0.43691	2.07E-09	3.65E-06	-0.32038	-0.37587
GOMF name	signaling receptor activity	34	-0.43700	1.23E-05	0.00272	-0.33494	-0.37928
GOMF name	phosphotransferase activity, alcohol group as acceptor	40	-0.44074	1.80E-06	0.00079	-0.30169	-0.37553
GOMF name	transmembrane signaling receptor activity	29	-0.45120	2.99E-05	0.00439	-0.34107	-0.38269
GOMF name	protein kinase activity	32	-0.46490	6.34E-06	0.00224	-0.33163	-0.40405
GOBP slim name	extracellular matrix organization	89	-0.47672	2.97E-14	2.82E-12	-0.38502	-0.48549
GOBP slim name	extracellular structure organization	89	-0.47672	2.97E-14	2.12E-12	-0.38502	-0.48549
GOBP slim name	biological adhesion	118	-0.50814	2.22E-20	6.34E-18	-0.34941	-0.39546
GOBP slim name	cell adhesion	118	-0.50814	2.22E-20	3.17E-18	-0.34941	-0.39546
GOCC slim name	extracellular matrix	55	-0.52077	4.45E-11	2.76E-09	-0.48351	-0.52832
GOCC slim name	transcription elongation factor complex	12	-0.52166	1.81E-03	0.01875	-0.28502	-0.29902
GOBP slim name	tissue remodeling	11	-0.52247	2.77E-03	0.03163	-0.43775	-0.37587
GOCC slim name	proteinaceous extracellular matrix	26	-0.55284	1.25E-06	3.11E-05	-0.52472	-0.55035
GOMF name	protein tyrosine kinase activity	15	-0.57832	1.12E-04	0.01319	-0.40430	-0.42201
GOBP slim name	cell growth	19	-0.58459	1.13E-05	0.00032	-0.44826	-0.49955

Type	Name	Size	Score	P value	Benj. Hoch. FDR	Mean	Median
GOMF name	transmembrane receptor protein tyrosine kinase activity	12	-0.59745	3.54E-04	0.03289	-0.41964	-0.44697
GOMF name	transmembrane receptor protein kinase activity	13	-0.62730	9.51E-05	0.01199	-0.46609	-0.47192
GOMF name	serine-type endopeptidase inhibitor activity	20	-0.63202	1.13E-06	0.00066	-0.46192	-0.46641
GOMF name	viral receptor activity	8	-0.74139	2.91E-04	0.03020	-0.48461	-0.51777
GOCC slim name	laminin complex	3	-0.77348	2.05E-02	0.09754	-0.52837	-0.48549
GOMF name	extracellular matrix structural constituent	13	-0.81452	4.03E-07	0.00036	-0.74888	-0.87111
GOMF name	transforming growth factor beta binding	6	-0.82419	4.83E-04	0.03872	-0.70383	-0.64495

Table S2: Differentially associated proteins in PSMD4 pull-down upon smoke exposure in murine lungs. Significant changes of five upregulated and 18 downregulated proteins from proteasome complexes in lungs of mice exposed to cigarette smoke for three days with two exposure cycles of 50 min/day.

UniProt Entry	Name		Unique peptides	Sequence coverage (%)	Stoichiometry to PSMD4 control	Stoichiometry to PSMD4 CS	Fold change CS/control	*p*-value
O09167	Rpl21	60S ribosomal protein L21	6	36.9	0.0922	0.1595	1.73	0.002
P26443	Glud1	Glutamate dehydrogenase 1, mitochondrial	18	36.7	0.0672	0.1135	1.65	0.024
Q9CVD2	Atxn3	Ataxin-3	6	24.2	0.0168	0.0271	1.59	0.038
P58252	Eef2	Elongation factor 2	6	8.6	0.0197	0.0296	1.48	0.011
Q9QXS6	Dbn1	Drebrin	7	14.4	0.0373	0.0483	1.30	0.025
P28063	Psmb8	Proteasome subunit beta type-8	13	48.2	0.5069	0.4511	0.89	0.043
P97470	Ppp4c	Serine/threonine-protein phosphatase 4 catalytic subunit	3	12.4	0.0160	0.0115	0.72	0.017
Q3TXS7	Psmd1	26S proteasome non-ATPase regulatory subunit 1	50	56.0	0.6424	0.4666	0.72	0.012
Q63918	Sdpr	Serum deprivation-response protein	25	53.1	0.2219	0.1499	0.68	0.022
P02469	Lamb1	Laminin subunit beta-1	5	3.1	0.0105	0.0068	0.64	0.012
P97927	Lama4	Laminin subunit alpha-4	3	2.2	0.0072	0.0045	0.62	0.002
Q3UGC7	Eif3j1	Eukaryotic translation initiation factor 3 subunit J-A	8	36.4	0.0572	0.0352	0.62	0.043
P02468	Lamc1	Laminin subunit gamma-1	10	7.1	0.0145	0.0088	0.60	0.015
P06684	C5	Complement C5	9	6.7	0.0303	0.0180	0.60	0.022
P21107	Tpm3	Tropomyosin alpha-3 chain	5	39.3	0.4643	0.2586	0.56	0.023
O54724	Ptrf	Polymerase I and transcript release factor	25	40.1	0.8629	0.4819	0.56	0.0004
P10493	Nid1	Nidogen-1	4	3.7	0.0076	0.0043	0.55	0.016
Q61838	Pzp	Pregnancy zone protein	9	6.8	0.1448	0.0784	0.55	0.016
Q8VDP4	Ccar2	Cell cycle and apoptosis regulator protein 2	2	2.0	0.0025	0.0014	0.54	0.020
P54726	Rad23a	UV excision repair protein RAD23 homolog A	2	10.5	0.0175	0.0092	0.52	0.022
P46735	Myo1b	Unconventional myosin-Ib	2	2.2	0.0011	0.0006	0.51	0.045
Q99K41	Emilin1	EMILIN-1	2	2.5	0.0049	0.0025	0.50	0.006
Q8R146	Apeh	Acylamino-acid-releasing enzyme	4	6.4	0.0138	0.0050	0.36	0.049

Table S3: Native MS analysis of isolated 20S proteasomes. The table summarizes the measured masses of the different 20S proteasome assemblies that were detected under the different treatments and HCD energies shown in Figure 4. Theoretical masses were calculated from the masses of the different 20S subunits, as detected in both the native and denaturative MS analyses. Charge denoted the most intense ion in each charge series.

Theoretical Masses	
Proteasome Type	**Mass (Da)**
alpha Ring (αR)	194,786
Half Proteasome (HP)	359,182
Full Proteasome (FP)	720,390
Stripped Proteasome (SP)	~ 690,000

HCD Energy (V)	**Control**				**25 % CSE 30min**				**50 % CSE 30min**			
	Measured Mass (Da)	**Error**	**Charge**	**Species**	**Measured Mass (Da)**	**Error**	**Charge**	**Species**	**Measured Mass (Da)**	**Error**	**Charge**	**Species**
0	716,748	11	+58	FP	706,302	110	+57	FP	726,890	191	+61	FP
25	716,978	119	+59	FP	717,341	123	+59	FP	718,706	118	+59	FP
50	715,412	53	+59	FP	716,393	127	+59	FP	726,598	37	+60	FP
75	724,744	48	+61	FP	700,983	128	+60	FP	736,085	115	+61	FP
	390,199	85	+42	HP	381,014	40	+41	HP	345,820	51	+37	HP
	194,851	26	+30	αR	194,939	23	+29	αR	195,898	45	+30	αR
100	710,553	138	+59	FP	710,731	60	+59	FP	697,998	111	+58	FP
	389,759	44	+42	HP	389,994	91	+42	HP	345,405	76	+38	HP
125	721,523	128	+60	FP	721,865	114	+41	FP	721,555	79	+61	FP
	389,693	33	+41	HP	390,938	69	+60	HP	390,708	56	+42	HP
150	721,300	57	+59	FP	721,534	66	+60	FP	721,360	89	+60	FP
									354,356	57	+40	HP
175	721,181	66	+57	FP	721,462	67	+58	FP	721,209	84	+60	FP
	693,860	44	+43	SP	694,127	29	+42	SP				
200	693,865	28	+41	SP								

SUPPLEMENTAL REFERENCES

[1] F.W. Studier, Protein production by auto-induction in high density shaking cultures, Protein Expr. Purif. 41 (2005) 207–234.

[2] H.C. Besche, W. Haas, S.P. Gygi, A.L. Goldberg, Isolation of Mammalian 26S Proteasomes and p97/VCP Complexes Using the Ubiquitin-like Domain from HHR23B Reveals Novel Proteasome-Associated Proteins, Biochemistry (Mosc.). 48 (2009) 2538–2549.

[3] S.M. Hauck, J. Dietter, R.L. Kramer, F. Hofmaier, J.K. Zipplies, B. Amann, A. Feuchtinger, C.A. Deeg, M. Ueffing, Deciphering membrane-associated molecular processes in target tissue of autoimmune uveitis by label-free quantitative mass spectrometry, Mol. Cell. Proteomics MCP. 9 (2010) 2292–2305.

[4] J.A. Vizcaíno, A. Csordas, N. del-Toro, J.A. Dianes, J. Griss, I. Lavidas, G. Mayer, Y. Perez-Riverol, F. Reisinger, T. Ternent, Q.-W. Xu, R. Wang, H. Hermjakob, 2016 update of the PRIDE database and its related tools, Nucleic Acids Res. 44 (2016) D447-456.

[5] A. Mossina, C. Lukas, J. Merl-Pham, F.E. Uhl, K. Mutze, A. Schamberger, C. Staab-Weijnitz, J. Jia, A.Ö. Yildirim, M. Königshoff, S.M. Hauck, O. Eickelberg, S. Meiners, Cigarette smoke alters the secretome of lung epithelial cells., Proteomics. (2016). doi: 10.1002/pmic.201600243.

[6] J. Merl, M. Ueffing, S.M. Hauck, C. von Toerne, Direct comparison of MS-based label-free and SILAC quantitative proteome profiling strategies in primary retinal Müller cells, Proteomics. 12 (2012) 1902–1911.

[7] B. Fabre, T. Lambour, D. Bouyssié, T. Menneteau, B. Monsarrat, O. Burlet-Schiltz, M.P. Bousquet-Dubouch, Comparison of label-free quantification methods for the determination of protein complexes subunits stoichiometry, EuPA Open Proteomics. 4 (2014) 82–86.

[8] M.Y. Hein, N.C. Hubner, I. Poser, F. Buchholz, A.A. Hyman, M.Y. Hein, N.C. Hubner, I. Poser, F. Buchholz, A.A. Hyman, M. Mann, A Human Interactome in Three Quantitative Dimensions Organized by Stoichiometries and Abundances, Cell. (2015) 712–723.

[9] G. Ben-Nissan, M.E. Belov, D. Morgenstern, Y. Levin, O. Dym, G. Arkind, C. Lipson, A.A. Makarov, M. Sharon, Triple-Stage Mass Spectrometry Unravels the Heterogeneity of an Endogenous Protein Complex, Anal. Chem. 89 (2017) 4708–4715.

[10] N. Kirshenbaum, I. Michaelevski, M. Sharon, Analyzing large protein complexes by structural mass spectrometry, J. Vis. Exp. JoVE. (2010) doi: 10.3791/1954.

[11] S. Rozen, A. Tieri, G. Ridner, A.-K. Stark, T. Schmaler, G. Ben-Nissan, W. Dubiel, M. Sharon, Exposing the subunit diversity within protein complexes: a mass spectrometry approach, Methods San Diego Calif. 59 (2013) 270–277.